Half-filled Hubbard model on a Bethe lattice with next-nearest-neighbor hopping

Robert Peters and Thomas Pruschke
Institute for Theoretical Physics, University of Göttingen, Friedrich-Hund-Platz 1, 37077 Göttingen, Germany
(Received 16 September 2008; revised manuscript received 15 October 2008; published 13 January 2009)

We study the interplay between Néel antiferromagnetism and the paramagnetic metal-insulator transition (PMIT) on a Bethe lattice with nearest- and next-nearest-neighbor hoppings t_1 and t_2. We concentrate in this paper on the situation at half-filling. For $t_2/t_1 \to 1$ the PMIT outgrows the antiferromagnetic phase and shows a scenario similar to V_2O_3. In this parameter regime we also observe another magnetic phase.

DOI: 10.1103/PhysRevB.79.045108 PACS number(s): 71.30.+h

I. INTRODUCTION

Understanding correlation effects is one major goal of condensed-matter physics. Strong correlations manifest themselves in various forms. The paramagnetic Mott-Hubbard metal-insulator transition (PMIT) (Ref. 1) is a well-known and interesting example. With increasing interaction strength the Fermi-liquid state breaks down at a critical value and an insulator is formed.

Another fundamental example is magnetism, where electrons reduce the energetic cost of the Coulomb interaction by ordering. Both effects can of course occur simultaneously and are the heart of the extremely rich phase diagram of, e.g., transition-metal compounds such as, for example, V_2O_3 or $LaTiO_3$.[2,3]

Besides strong correlations, another major ingredient for the understanding of the phase diagram of compounds such as V_2O_3 is frustration. V_2O_3 crystallizes in the corundum structure with the V ions located on a honeycomb lattice in the *ab* plane while along the *c* axis a more complicated coordination is observed, which induces frustration of the magnetic interactions.[1] Nevertheless the phase diagram of V_2O_3 does show an antiferromagnetic phase at temperatures below $T_N \approx 180$ K. Upon doping with Ti, one may suppress this order. Such a doping with a smaller ion can be viewed as internal pressure;[1] hence the suppression of the magnetic order is commonly interpreted as happening through an increase in the bandwidth, or equivalently, a decrease in the correlation effects. Consequently, the critical Ti doping is conventionally related to the existence of a lower critical value of the electronic interaction parameter. At higher temperatures the antiferromagnetic state becomes unstable toward a paramagnet and one can eventually observe a paramagnetic metal-insulator transition (MIT) up to temperatures $T \approx 400$ K.

Frustration is quite a common feature in real materials. Very interesting examples for frustrated systems are layered organic compounds such as κ-(BEDT-TTF)2X.[4–17] They have a similar phase diagram as the high-temperature superconductors (HTSCs).[18] The phases of these organic systems are controlled by pressure and frustration rather than by doping as in HTSC.[19] They are usually described by an anisotropic triangular lattice, and changing the anion (*X*) in these systems modifies the frustration of the lattice. Besides superconductivity, magnetic ordering and a PMIT can also be found.

These two examples by no means exhaust the zoo of materials, showing such interplay or competition between PMIT and ordered phases.[1] For example, rare-earth compounds such as $Ce(Rh,Ir)_{1-x}(Co,Ir)_xIn_5$ do show a similarly bizarre phase diagram.[20] Besides their usually complicated lattice structure, another challenge for a theoretical description of such compounds is that the presence of elements with partially filled *d* or *f* shells in principle requires a multiorbital description to account for effects such as Hund's or spin-orbit coupling properly. Furthermore the residual degeneracies in the solid-state crystalline environment lead to degenerate multiplets which in turn can give rise to even more complex structures such as orbital order or polaron formation (see, e.g., Imada *et al.*[1] for an overview and references).

Although all these ingredients play an important role for a quantitative theoretical description of transition-metal or rare-earth compounds, we here want to focus on the one-orbital situation, in particular on the relation between PMIT and antiferromagnetism. This restriction to a simpler but by no means trivial situation will enable us to investigate the relation between these two paradigms of correlation effects with a small and controllable set of parameters and thus obtain some hint to how both phases interact. A model suitable for analyzing this kind of physics is provided through the Hubbard model,[21–23]

$$H = \sum_{i,j,\sigma} t_{ij} c^\dagger_{i\sigma} c_{j\sigma} + U \sum_i n_{i\uparrow} n_{i\downarrow}, \tag{1}$$

where $c^\dagger_{i\sigma}(c_{i\sigma})$ creates (annihilates) an electron with spin σ at site i and $n_{i\uparrow}(n_{i\downarrow})$ is the density operator for spin up (spin down) at site i. The parameters t_{ij} represent the hopping amplitude from i to j and U is the interaction strength. In this paper we will measure the interaction relative to the bandwidth, which is related to the hopping amplitude. Although, at first sight, very simplistic, this model is highly nontrivial. Besides other methods, especially in one dimension, progress in understanding its physics was achieved by the development of the dynamical mean-field theory (DMFT).[24] The DMFT is a very powerful tool for analyzing strongly correlated lattice systems, mapping the lattice problem onto a quantum impurity problem, which has to be solved self-consistently. For solving this impurity problem for arbitrary interaction strengths and temperatures, we here use Wilson's numerical renormalization group (NRG).[25,26] An interesting fact is that the only information about the lattice structure, which enters a DMFT self-consistency calculation, is the lo-

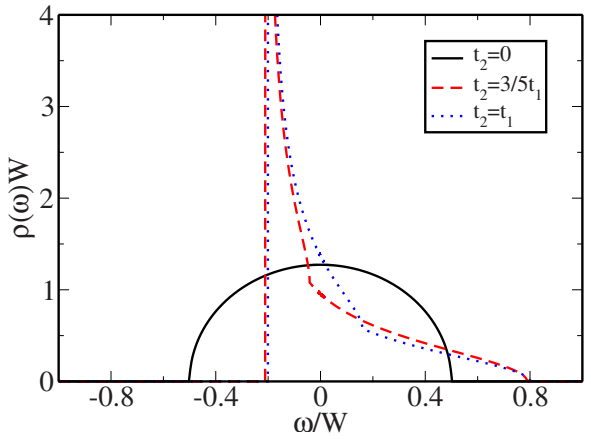

FIG. 1. (Color online) DOS for increasing NNN hopping t_2. Observe the van Hove singularity at the lower band edge. $\rho(\omega)$ and ω are scaled with the bandwidth $W=4t_2+2t_1+t_1^2/(4t_2)$ $(t_2>1/4t_1)$.

cal density of states (DOS) of the noninteracting system. We performed our calculations for a Bethe lattice with nearest-neighbor (NN) and next-nearest-neighbor (NNN) hoppings t_1 and t_2, respectively. The DOS in this case can be calculated using a topological ansatz.[27,28] Starting from a particle-hole symmetric DOS at $t_2=0$, the density of states becomes now asymmetric with increasing t_2 (see Fig. 1) and develops a van Hove singularity at the lower band edge for positive and increasing NNN hopping t_2. In contrast to $t_2=0$, where the particle-hole symmetry can be employed to fix the filling at $\langle n\rangle=1$ precisely, the asymmetry present for $t_2\neq 0$ makes it more difficult to perform calculations with the filling kept at $\langle n\rangle=1$ with sufficient accuracy. Thus DMFT calculations typically take much longer here due to the necessary adjustment of the chemical potential. Of course the Bethe lattice does not represent a lattice realized in real materials. However, in contrast to the hypercubic lattice with infinite coordination number, the Bethe lattice has a compact support and thus possesses band edges, which provides a more realistic scenario.

Since the early days of DMFT, there have been many contributions by different groups to the subject of the PMIT and antiferromagnetism.[24,29] However, frustration effects up to now where introduced in DMFT typically within the so-called two-sublattice fully frustrated model,[24,30–34] which results in a particle-hole symmetric DOS even with frustration. As a side effect, this way of introducing frustration leaves the paramagnetic phase unchanged. For the nonfrustrated system the PMIT is then completely covered by the antiferromagnetic phase, which exists for half-filling for all finite values of U.[29,35] For the frustrated system, on the other hand, there exists a lower critical value for the interaction U, which increases with increasing frustration. It was furthermore found that the Néel temperature decreases with increasing frustration such that the PMIT outgrows the antiferromagnetic phase.[34] In early calculations using this way of introducing frustration based on exact diagonalization studies of the two-sublattice fully frustrated model,[24,32,33] the authors also found parameter regions in the phase diagram where an antiferromagnetic metal appeared to be stable. However, this antiferromagnetic metal phase was later traced back to numerical subtleties in the exact diagonalization procedure and shown to be actually absent from the phase diagram.[34]

An attempt to study the Hubbard model on the Bethe lattice with correct inclusion of NN and NNN hoppings has been performed rather recently.[36] In this work the authors concentrated on the paramagnetic PMIT and found phase separation between the insulating and metallic phases.

In this paper we investigate the PMIT as well as antiferromagnetism and concentrate on the competition between the paramagnetic phase including the PMIT and the antiferromagnetic phase at intermediate and high grades of frustration. We especially look at the case $t_2\rightarrow t_1$ and raise the question: does the scenario of the outgrowing PMIT, proposed by Zitzler *et al.*,[34] still holds for the correct asymmetric density of states? The paper is arranged as follows. After this introduction we start with a brief look at the PMIT, followed by a discussion of the phase diagram at half-filling including antiferromagnetism and the PMIT. Section IV addresses especially the case of very strong frustration and the question on how the magnetic order is realized there. The paper will be closed by a summary of our results and an outlook.

II. METAL-INSULATOR TRANSITION

The metal-insulator transition for the Bethe lattice with NNN hopping has been analyzed by Eckstein *et al.*[36] within the self-energy functional approach.[37] They particularly focused on $t_2/t_1=3/7$ and discussed an unexpected occurrence of phase separation in the paramagnetic state between a Mott-Hubbard insulator and a correlated metal at and near half-filling. Here we want to investigate the behavior of the system as a function of increasing frustration. Due to symmetry there is no difference between t_2 and $-t_2$. The calculations were done using Wilson's NRG as impurity solver for the DMFT, with $\Lambda=2$ and 1800 states kept per NRG step, and a logarithmic broadening $b=0.8$ to obtain spectral functions. We want to note at this point that the choice of NRG numerical parameters does not influence the qualitative nature of the results. We observe, however, small dependencies on Λ and b, which tend to become more pronounced when close to phase transitions and may result in systematic errors in numerical values for critical parameters of the order of $<5\%$.[26]

Figure 2 shows the paramagnetic metal-insulator transition for various values t_2/t_1. As energy scale we choose the bandwidth

$$W=\begin{cases}4t_1 & \text{for } 0\leq|t_2|\leq t_1/4\\ 4|t_2|+2t_1+t_1^2/(4|t_2|) & \text{for } |t_2|>t_1/4\end{cases}$$

of the noninteracting system. Note that these results are obtained by artificially suppressing an antiferromagnetic instability. We will come back to this point later. The occupation was kept fixed at $n=1\pm 0.005$ by adjusting the chemical potential. Note that in contrast to the case with $t_2=0$ it is not possible to achieve $n=1$ here within numerical precision due to the asymmetric DOS (see Fig. 1). For increasing $t_2/t_1\rightarrow 1$ the PMIT is shifted toward lower interaction strengths

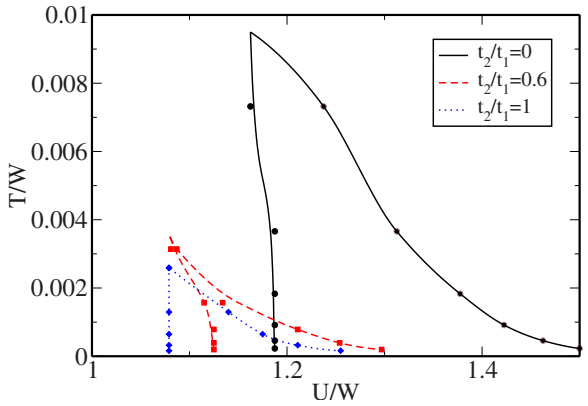

FIG. 2. (Color online) The transition lines for the PMIT for different frustrations as a function of temperature and interaction strength. For each frustration the right line represents the transition from the metal to the insulator while the left line represents the transition from the insulator to the metal. Symbols mark the calculated data points, in which the lines are fits meant as guide for the eyes.

and also lower temperatures. While the shift in the interaction strength is rather moderate, we notice a large difference in the temperature of the critical end point between the unfrustrated and highly frustrated systems. This observation of course renews our interest in the question: to what extent can long-range hopping help in pushing the paramagnetic MIT out of the expected antiferromagnetic phase for reasonable magnitudes of t_2 to create a phase diagram similar to the one found for V_2O_3? The scenario proposed by Zitzler *et al.*[34] relied on the fact that the paramagnetic phase largely remains unaltered with increasing t_2. As the Néel temperature for the antiferromagnet is reduced at the same time, the PMIT can eventually outgrow the antiferromagnetic phase.

III. ANTIFERROMAGNETISM AT FINITE t_2

We now allow for antiferromagnetic ordering in our calculations. To this end we reformulate the DMFT for an *AB* lattice structure[24,29] to accommodate the Néel ordering and initialize the calculation with a small staggered field, which is turned off after one DMFT iteration. The system then either evolves into a paramagnetic or antiferromagnetic state with increasing number of DMFT iterations. Figure 3 shows the resulting phase diagrams for $t_2/t_1=0.6$ (left panel) and $t_2/t_1=0.8$ (right panel) for different temperatures and interaction strengths. The small black points show the locations, where calculations have actually been performed. From these data the shaded areas were constructed representing the antiferromagnetic phases. This of course means that the phase boundaries shown here must be considered as guess only. However, as we do not expect any strange structures to appear, this guess will presumably represent the true phase boundary within a few percent.

The full lines in Fig. 3 are the PMIT transitions. Note that for both diagrams the same division of axes was chosen.

In contrast to the Hubbard model on a bipartite lattice with $t_2=0$, there now exists a finite critical value U_c^{AF}, below which no antiferromagnetism can be stabilized even for temperature $T\rightarrow 0$. With increasing frustration the paramagnetic-antiferromagnetic transition is shifted toward higher interaction strengths and lower temperatures while the PMIT is shifted toward lower interaction strengths. So obviously the PMIT is shifted toward the phase boundaries of the antiferromagnetic dome. So far this is the expected effect of the NNN hopping which introduces frustration to the antiferromagnetic exchange. However, note that, although $t_2/t_1=0.8$ represents already a very strongly frustrated system, the PMIT still lies well covered within the antiferromagnetic phase.

Let us now have a closer look at the paramagnetic-antiferromagnetic transition. Here, Zitzler *et al.*[34] made the prediction that one has to expect a first-order transition close to the critical U_c^{AF} at low temperatures while at larger values of U again a second-order transition was found.

Figure 4 shows the staggered magnetization for different temperatures and interaction strengths at fixed $t_2/t_1=0.8$. The upper panel collects data for the transition at low temperatures at the lower edge of the antiferromagnetic phase. The full lines represent the transition from the paramagnetic to the antiferromagnetic state with increasing interaction

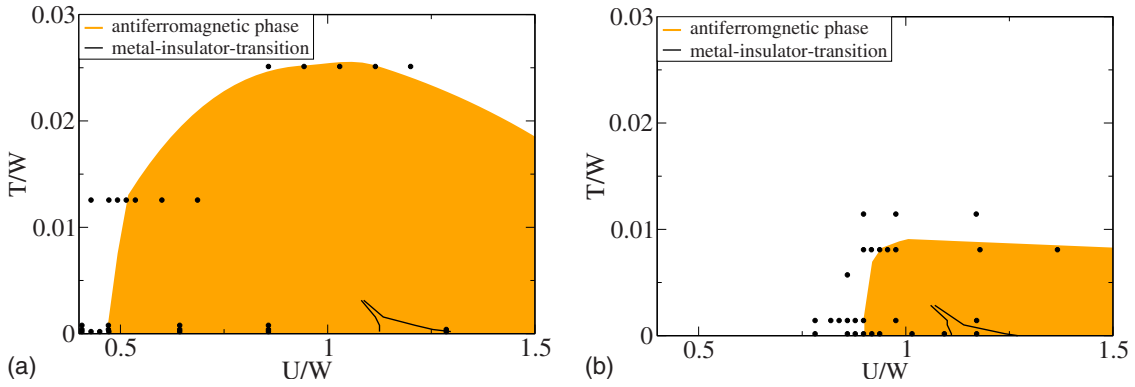

FIG. 3. (Color online) The left (right) panel shows the $T-U$ phase diagram for $t_2/t_1=0.6$ (0.8). The shaded area represents the antiferromagnetic phase while the white area represents the paramagnetic phase. The lines show where the PMIT in the paramagnetic phase would occur. The points denote the parameter values, where DMFT calculations were done. From these points the shaded area was constructed as guide for the eyes. Additional calculations were performed to find the PMIT lines.

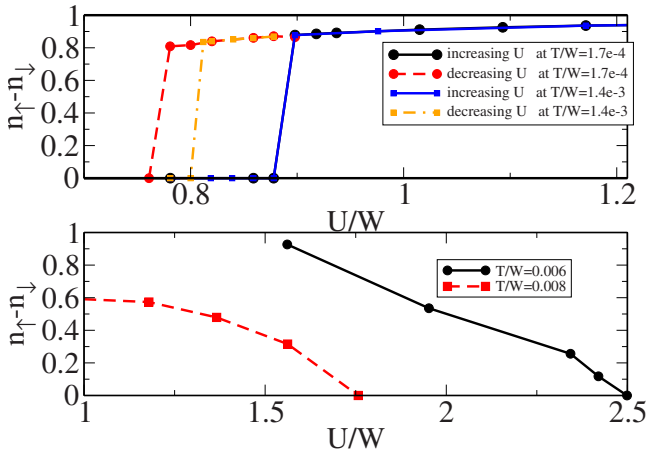

FIG. 4. (Color online) Staggered magnetization versus interaction U/W for two different temperatures and $t_2/t_1=0.8$. In the upper panel there are for each temperature two transition lines, representing either increasing or decreasing interaction strength. The region between both lines embodies a hysteresis region. The lower panel shows the transition for large interaction strengths. Here no hysteresis region could be found but a smooth transition.

strength for two different temperatures while the dashed lines represent the transitions from the antiferromagnetic to the paramagnetic state with decreasing interaction strength. In the upper panel (small U) one can clearly see a hysteresis of the antiferromagnetic transition. This hysteresis and the jump in the magnetization are clear signs for a first-order transition. This antiferromagnetic hysteresis is very pronounced for strong frustration but numerically not resolvable for example for $t_2/t_1=0.2$. We believe that the hysteresis region shrinks with decreasing t_2 and eventually cannot be resolved anymore with numerical techniques. The whole temperature-dependent hysteresis region can be seen in Fig. 5 for the case $t_2/t_1=0.8$. One can see clearly the shrinking of the hysteresis region with increasing temperature. Note that such a hysteresis is also found in the two-sublattice fully frustrated model,[34] which means that this quite likely is a generic effect

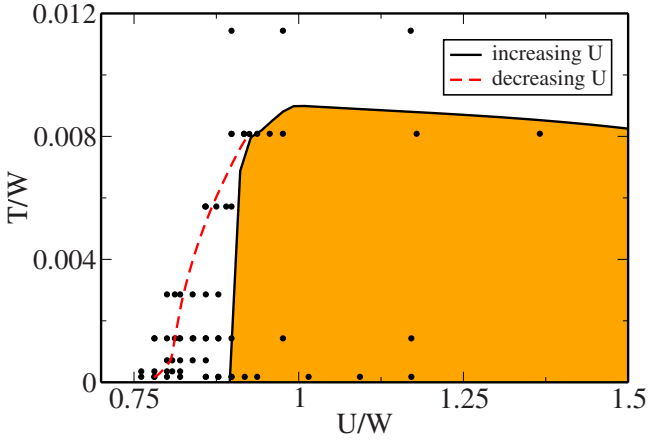

FIG. 5. (Color online) Phase diagram for $t_2/t_1=0.8$ including the temperature depending hysteresis region (between dashed and full lines). The meaning of symbols is the same as in Fig. 3. The shaded area is the same as before meant as guide for the eyes.

in frustrated systems at intermediate coupling strengths.

The lower panel in Fig. 4 shows the staggered magnetization for temperatures just below the corresponding Néel temperatures and at large interaction strengths. Here the magnetization vanishes smoothly, which is the behavior expected for a second-order phase transition. In summary we thus find a first-order transition at the critical interaction U_c^{AF} where antiferromagnetism sets in, and a second-order transition for the large Coulomb parameter $U \gg W$. The merging from both transition lines is an interesting point in itself. There must be a critical point where the first-order transition changes into a second-order transition. It is however not possible to resolve this merging within DMFT/NRG. First, the logarithmic discretization of the temperatures within the NRG does not allow resolving of this merging region with arbitrary precision. Second, the magnetization of the system becomes very small in this region so it is not possible to distinguish between a (tiny) jump and numerical artifacts of a smoothly vanishing order parameter. Consequently, we cannot decide anymore of what order the transition will be.

Antiferromagnetic metallic phases at half-filling were reported in earlier publications.[30–33] In our calculations we saw no evidence for an antiferromagnetic metallic state at half-filling. Especially for strong frustration $t_2/t_1 \approx 0.8$, the system directly jumps from a paramagnetic metallic solution into an antiferromagnetic insulating solution with high magnetization. In the papers cited, the region showing an antiferromagnetic metallic solution broadens with increasing t_2. We clearly cannot confirm this prediction, as discussed above. Only in systems with small to intermediate frustration there are narrow interaction regimes where we observe a small finite weight at the Fermi level. One must however consider that the occupation number is not exactly one but only within 0.5%. Also it was sometimes difficult to stabilize a DMFT solution in these regions. In summary, we cannot see any clear signs for an antiferromagnetic metallic state at half-filling in our calculations. If any exists, it can only be found in rather low frustration in a very small regime about the critical interaction. To what extent these rather special conditions can then be considered as realistic for real materials is yet another question.

IV. NEARLY FULLY FRUSTRATED SYSTEM

In this section we want to study the situation in which t_1 and t_2 are comparable in strength. Interestingly, there has been no attempt to calculate the phase diagram on a mean-field level in the strongly frustrated model $t_2 \approx t_1$. Therefore, before discussing the results of the DMFT calculations for strongly frustrated systems $t_2/t_1 \approx 1$, let us try to gain some insight into the physics we must expect by inspecting classical spins on a Bethe lattice with NN interaction J_1 and NNN interaction J_2. Allowing that nearest-neighbor spins enclose an angle θ, one ends up with the energy functional

$$E/2N = J_1 Z \cos(\theta) + J_2 Z \sum_{i=1}^{Z-1} [\cos(\theta)^2 + \sin(\theta)^2 \cos(2\pi i/Z)]. \tag{2}$$

Performing the same limits and scaling as in DMFT, one finds (see Appendix)

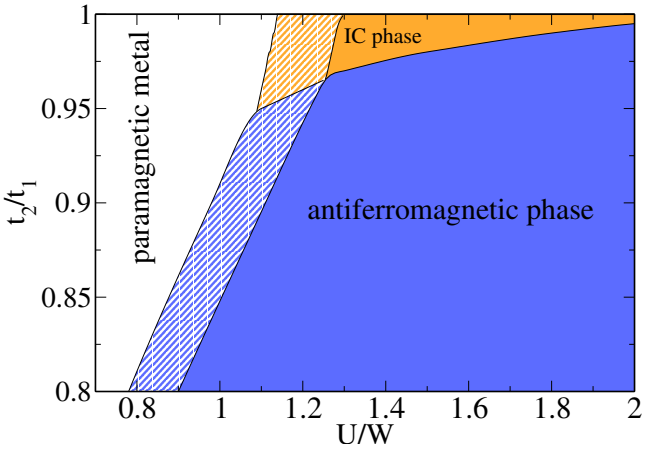

FIG. 6. (Color online) Ground state ($T=0$) phase diagram for different strengths of frustration as a function of the interaction. The brindled regions are hysteresis regions for increasing or decreasing interaction. The phase boundaries of the IC phase are only qualitative (for explanation, see text).

$$E/2N = J_1 \cos(\theta) + J_2 \cos(\theta)^2. \tag{3}$$

Thus, the Néel state with $\theta=\pi$ is the stable ground state for $J_2<\frac{1}{2}J_1$ while one finds a spin wave with $\theta=\pi - \arccos(J_1/2J_2)$ for $J_2>\frac{1}{2}J_1$.

For the DMFT calculations we can allow only for solutions commensurate with the lattice. This however will possibly be inconsistent with the spin structure favored by the system. If, for example, we perform a calculation focusing on the ferromagnetic solution within a parameter regime, where the system wants to order antiferromagnetically, DMFT will not converge. To investigate spin-wave states with periodicities with more than two lattice sites, one has to set up the correct DMFT self-consistency equations respecting the lattice structure. While, for a system on an infinite Bethe lattice with NN hopping only, it is straightforward to extend the DMFT to commensurate magnetic structures with periodicities of more than two lattice sites, we did not succeed in devising a scheme that allows for such calculations for systems with NNN hopping. The reason is that one has to partition the lattice into an *ABCD*… structure. However, the NNN hopping makes it impossible to uniquely identify the connectivity of the respective sublattices. A method proposed by Fleck *et al.*[38] for the two-dimensional cubic lattice is not applicable in our case.

We thus only allowed for paramagnetic, ferromagnetic, and antiferromagnetic solutions in our calculations. The resulting phase diagrams for $t_2 \to t_1$ are shown in Figs. 6 and 7. Figure 6 displays the ground states for different grades of frustration and interaction strengths. For $t_2/t_1<0.95$ the phase diagram has the same structure as for small and intermediate t_2. The critical interaction strength U_c^{AF} necessary to stabilize the Néel state increases and for all values above U_c^{AF}, we find an antiferromagnetic phase with a hysteresis region at the phase boundary. For $0.95<t_2/t_1<1$ the critical value U_c^{AF} one needs to stabilize the Néel state increases dramatically. For $t_2=t_1$ finally we do not find an antiferromagnetic Néel state at all for any interaction strength U. Our

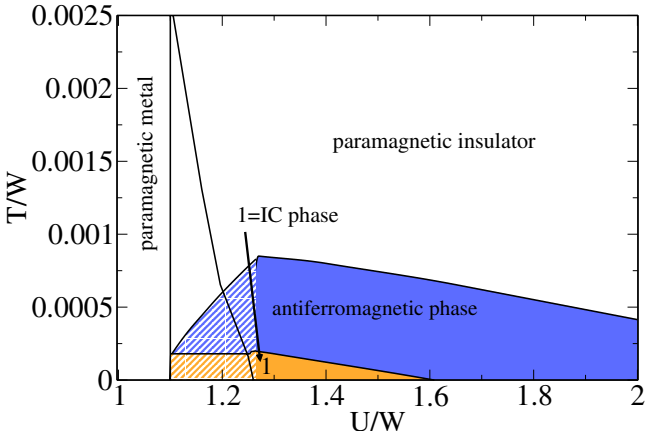

FIG. 7. (Color online) Phase diagram $T-U$ for $t_2/t_1=0.98$ including the PMIT. The brindled area represents again the hysteresis region.

DMFT calculations however indicate that in this range of t_2/t_1 there actually does exists another magnetic phase. Namely, for sufficiently small temperatures, one obtains a finite spin polarization in every DMFT iteration. However, the DMFT does not converge to a unique state as a function of DMFT iterations (see also Fig. 8). In the phase diagrams in Figs. 6 and 7 we have named this regime the incommensurate phase (IC phase). In this parameter regime the Néel state becomes unstable toward the behavior shown in Fig. 8. Here one can switch between a conventional Néel state and the IC phase by only a small change in the interaction strength. Note, that the phase boundaries shown in the figure must be taken with some care as we cannot compare the energies of the Néel state and this IC phase to properly determine the phase boundaries. As we observe precisely the same behavior for all investigated values $t_2/t_1 = \{0.96, 0.97, 0.98, 0.99, 1.0\}$, we are convinced that the ground state in this region is an incommensurate state, as to be expected from our results for $S=\infty$. Similar observations also hold for finite temperatures as shown in Fig. 7, where

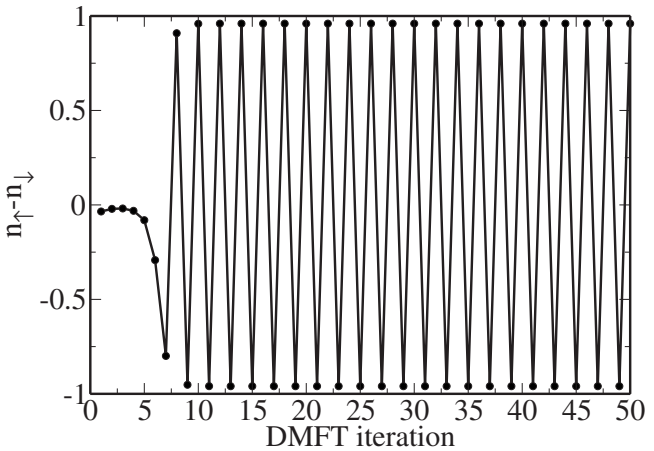

FIG. 8. Example of a nonconvergent DMFT calculation. The figure shows the staggered polarization over the DMFT iteration number for $t_2/t_1=0.98$, $U/W=1.35$, and $T\approx 0$. The lines are meant as guide for the eyes.

the $T-U$ phase diagram for fixed $t_2/t_1=0.98$ is displayed. For increasing interactions and $T=0$, there first is a transition from a paramagnetic metal to the IC phase and for $U/W \approx 1.6$ from the IC phase to the Néel state. For increasing temperature the IC phase eventually becomes unstable toward the Néel state. In Fig. 7 one can also see the PMIT lines. As one can see it lies within the hysteresis region of the magnetic phases but clearly outgrows both magnetic phases. This is the scenario described in Zitzler *et al.*[34]

V. SUMMARY

We studied the DMFT phase diagram of the Hubbard model at half-filling in the presence of NN and NNN hoppings. In contrast to previous investigations we did our calculations for a Bethe lattice with proper NNN hopping t_2, introducing a highly asymmetric DOS already for the noninteracting system. The first important observation concerns the paramagnetic metal-insulator transition, which is suppressed by increasing t_2 but at the same time shifted to lower values of the Coulomb interaction.

At $t_2=0$ the ubiquitous antiferromagnetic phase on the other hand is suppressed up to a critical value $U_c^{\mathrm{AF}}(t_2)$ with increasing t_2, as expected. Furthermore, a hysteresis region between the paramagnetic metal at small U and the antiferromagnetic insulator at large U develops, showing that the transition is of first order. Note that we did not observe any evidence for an antiferromagnetic metal close to the phase boundary nor did the PMIT reach out of the antiferromagnetic insulator up to values $t_2=0.8t_1$.

Thus far the observations are similar to the results found by Zitzler *et al.*[34] for the two-sublattice fully frustrated Bethe lattice.[24] The shift of the PMIT to lower values of U together with a moderate suppression of the critical temperature for larger t_2 however motivated a more detailed investigation of the region of larger t_2. A simple argument based on classical spins with competing interactions showed that one has to expect an additional incommensurate phase here. In fact, as already anticipated qualitatively by Zitzler *et al.*,[34] for frustrations $0.96<t_2/t_1<1.0$, we eventually found that the PMIT lies within the hysteresis region of the antiferromagnetic phase for $T=0$ but outgrows it in temperature. For such strong frustration we also found evidence for another magnetic phase besides ferromagnetism or antiferromagnetism. Unfortunately this phase could not be stabilized within our DMFT calculations so its real nature remains open. In connection with our argument based on classical spins, we believe that we can interpret the observed structure as an incommensurate phase. This conjecture is further supported by the fact that for $t_1=t_2$ we found no antiferromagnetic solution of the Néel type but only this frustrated magnetic phase. Especially the latter findings make it highly desirable to set up a scheme that allows studying of commensurable structures with period beyond Néel type for arbitrary lattice structures including longer-ranged hopping.

ACKNOWLEDGMENTS

We want to thank Martin Eckstein and Markus Kollar for many helpful discussions on the Bethe lattice with NNN hopping and Timo Aspelmeier for his help with the vector spins. This work was supported by the DFG through Contract No. PR298/10. Computer support was provided by the Gesellschaft für Wissenschaftliche Datenverarbeitung in Göttingen and the Norddeutsche Verbund für Hoch-und Höchstleistungsrechnen.

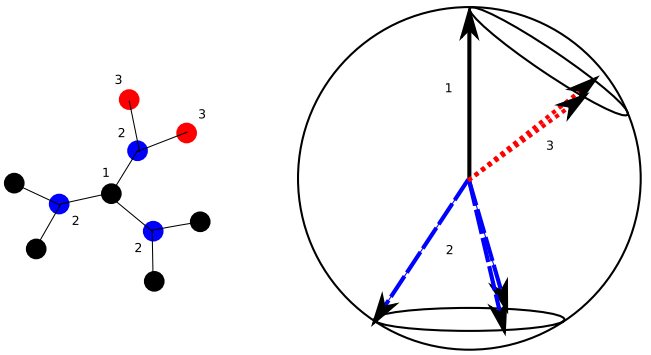

FIG. 9. (Color online) Left: Bethe lattice $Z=3$ with sites numbered according to the vector spins on the right. The nearest neighbors of site 1 must lie on a circle so there is an angle θ between 1 and 2. Similarly the nearest neighbors of one of the two spins must lie on a circle including the three spins and the one spin.

APPENDIX: CALCULATION FOR VECTOR SPINS

Here we want to present the calculation for three-dimensional vector spins on a Bethe lattice with antiferromagnetic coupling between NN- and NNN-lattice sites. We take Z nearest neighbors and interaction strengths J_1 between NN sites and J_2 between NNN sites. The last parameter entering this calculation is the angle θ between NN spins. Although the initial assumption that two neighboring spins form an angle theta may seem somewhat restrictive, we are not aware of other configurations with lower total energy.[39] We want to minimize the energy with respect to this angle. According to Fig. 9 the NN spins of one spin, must lie on a circle. The spins ending on the circle are all NNN spins. Due to the antiferromagnetic interaction J_2, we assume that they want to maximize the angle between them. Since there are Z spins on each circle, we assume they will have angle $2\pi/Z$ projected on the circle. Using now simple trigonometry, the angle between NNN spins is given by

$$\cos\gamma = \frac{2-[2R^2-2R^2\cos(2\pi i/Z)]}{2}$$

$$= \cos(\theta)^2 + \sin(\theta)^2\cos(2\pi i/Z),$$

where i runs from 0 to $Z-1$, giving different positions on one circle. Inserting this into the Hamiltonian

$$E = J_1 \sum_{i,j\in \mathrm{NN}} \vec{S}_i\vec{S}_j + J_2 \sum_{i,j\in \mathrm{NNN}} \vec{S}_i\vec{S}_j,$$

one finds for the energy

$$E/2N = J_1 Z \cos(\theta) + J_2 Z \sum_{i=1}^{Z-1} [\cos(\theta)^2 + \sin(\theta)^2 \cos(2\pi i/Z)].$$

Performing now the limit $Z \to \infty$ and scaling $J_1 Z \to J_1^\star$ and $J_2 Z \to J_2^\star / Z$, one finally obtains for the energy per lattice site

$$E_{Z=\infty}(\theta)/(2N) = J_1^\star \cos(\theta) + J_2^\star \cos(\theta)^2.$$

One can now see that the Néel state $\theta = \pi$ is stable for $J_2^\star / J_1^\star < 1/2$ because $d^2 E(\theta = \pi)/d\theta^2 = J_1^\star - 2J_2^\star$.

[1] M. Imada, A. Fujimori, and Y. Tokura, Rev. Mod. Phys. **70**, 1039 (1998).
[2] D. B. McWhan, J. P. Remeika, W. F. Brinkman, and T. M. Rice, Phys. Rev. B **7**, 1920 (1973).
[3] T. Katsufuji, Y. Taguchi, and Y. Tokura, Phys. Rev. B **56**, 10145 (1997).
[4] S. Lefebvre, P. Wzietek, S. Brown, C. Bourbonnais, D. Jérome, C. Mézière, M. Fourmigué, and P. Batail, Phys. Rev. Lett. **85**, 5420 (2000).
[5] S.-W. Tsai and J. Marston, Can. J. Phys. **79**, 1463 (2001).
[6] H. Morita, S. Watanabe, and M. Imada, J. Phys. Soc. Jpn. **71**, 2109 (2002).
[7] Y. Kurosaki, Y. Shimizu, K. Miyagawa, K. Kanoda, and G. Saito, Phys. Rev. Lett. **95**, 177001 (2005).
[8] T. Sasaki, N. Yoneyama, A. Suzuki, N. Kobayashi, Y. Ikemoto, and H. Kimura, J. Phys. Soc. Jpn. **74**, 2351 (2005).
[9] K. Aryanpour, W. E. Pickett, and R. T. Scalettar, Phys. Rev. B **74**, 085117 (2006).
[10] H. Yokoyama and M. Ogata, and Y. Tanaka, J. Phys. Soc. Jpn. **75**, 114706 (2006).
[11] B. Kyung and A.-M. S. Tremblay, Phys. Rev. Lett. **97**, 046402 (2006).
[12] T. Watanabe, H. Yokoyama, Y. Tanaka, and Jun-ichiro Inoue, J. Phys. Soc. Jpn. **75**, 074707 (2006).
[13] T. Koretsune, Y. Motome, and A. Furusaki, J. Phys. Soc. Jpn. **76**, 074719 (2007).
[14] T. Watanabe, H. Yokoyama, Y. Tanaka, and J. Inoue, Phys. Rev. B **77**, 214505 (2008).
[15] T. Ohashi, T. Momoi, H. Tsunetsugu, and N. Kawakami, Phys. Rev. Lett. **100**, 076402 (2008).
[16] T. Sasaki, N. Yoneyama, and N. Kobayashi, Phys. Rev. B **77**, 054505 (2008).
[17] A. H. Nevidomskyy, C. Scheiber, D. Senechal, and A.-M. S. Tremblay, Phys. Rev. B **77**, 064427 (2008).
[18] R. McKenzie, Science **278**, 820 (1997).
[19] P. Lee, N. Nagaosa, and X.-G. Wen, Rev. Mod. Phys. **78**, 17 (2006).
[20] H. Hegger, C. Petrovic, E. G. Moshopoulou, M. F. Hundley, J. L. Sarrao, Z. Fisk, and J. D. Thompson, Phys. Rev. Lett. **84**, 4986 (2000).
[21] J. Hubbard, Proc. R. Soc. London, Ser. A **276**, 238 (1963).
[22] J. Kanamori, Prog. Theor. Phys. **30**, 275 (1963).
[23] M. C. Gutzwiller, Phys. Rev. Lett. **10**, 159 (1963).
[24] A. Georges, G. Kotliar, W. Krauth, and M. J. Rozenberg, Rev. Mod. Phys. **68**, 13 (1996).
[25] K. G. Wilson, Rev. Mod. Phys. **47**, 773 (1975).
[26] R. Bulla, T. A. Costi, and T. Pruschke, Rev. Mod. Phys. **80**, 395 (2008).
[27] M. Kollar *et al.*, Ann. Phys. **14**, 642 (2005).
[28] M. Eckstein, M. Kollar, K. Byczuk, and D. Vollhardt, Phys. Rev. B **71**, 235119 (2005).
[29] T. Pruschke, Prog. Theor. Phys. **160**, 274 (2005).
[30] M. J. Rozenberg, G. Kotliar, H. Kajueter, G. A. Thomas, D. H. Rapkine, J. M. Honig, and P. Metcalf, Phys. Rev. Lett. **75**, 105 (1995).
[31] D. Duffy and A. Moreo, Phys. Rev. B **55**, R676 (1997).
[32] W. Hofstetter and D. Vollhardt, Ann. Phys. **7**, 48 (1998).
[33] R. Chitra and G. Kotliar, Phys. Rev. Lett. **83**, 2386 (1999).
[34] R. Zitzler, N.-H. Tong, T. Pruschke, and R. Bulla, Phys. Rev. Lett. **93**, 016406 (2004).
[35] P. G. J. van Dongen, Phys. Rev. Lett. **67**, 757 (1991).
[36] M. Eckstein, M. Kollar, M. Potthoff, and D. Vollhardt, Phys. Rev. B **75**, 125103 (2007).
[37] M. Potthoff, Eur. Phys. J. B **32**, 429 (2003).
[38] M. Fleck, A. I. Lichtenstein, A. M. Oles, and L. Hedin, Phys. Rev. B **60**, 5224 (1999).
[39] T. Aspelmeier (private communication).